CONCEPTUAL MODELING OF A DEEP SEATED NAPL DEPOSIT IN VOLCANOGENIC ROCKS

Alexey V. Kiryukhin

Institute of Volcanology and Seismology FEB RAS
Piip-9
Petropavlovsk-Kamchatsky, Russia
e-mail: avk2@kscnet.ru

ABSTRACT

A NAPL-bearing volcanogenic reservoir exists in West Siberia, hosted in Triassic age rocks (rhyolite tuffs) at a depth between 2.5 and 2.8 km, overlaid by low-permeable clay-argillite formations. Reservoir temperatures range from 120 to 130 ^{o}C, and pressures from 290 to 310 bars. Integrated analysis of the geological and geophysical data shows circulation patterns, where upflow zones can be identified by positive temperature and pressure anomalies, while downflows lead to negative anomalies. Those circulation patterns coincide with the former Triassic volcanoe vents, which are related to volcanic breccias.

Conceptual TOUGH-modeling was used to verify the possibility of a NAPL deposit accumulation in the clay overlaying the Triassic rhyolite tuffs reservoir. This deposit is fed by NAPL bearing upflows from buried volcanic vents. In a first step, a 3D numerical model of the reservoir was developed, covering 10 × 8 × 3 km^3, and discretized by rectangular 10 × 8 × 30 grid. Inverse iTOUGH2-EOS1-modeling was used to estimate heat and mass flows as well as permeabilities. Next, direct T2VOC modeling was used to reproduce the NAPL distribution in the volcanogenic reservoir. NAPL phase saturations matched the reservoir exploration data. In parallel to conceptual modeling, iTOUGH2-EOS3 was used to estimate thermal properties of reservoir rocks (heat conductivity and specific heat) based on laboratory heat tests data performed on rock samples.

INTRODUCTION

Papers presented at WGC-2005 and previous publications show that most of the high-temperature geothermal fields occur in various hydrogeological structures of recent volcanic areas: 1. Basins of the Quaternary stratovolcanoes and shield volcanoes (15% of the world geothermal electricity production); 2. Contact zones of the Quaternary intrusions and dyke swarms hosted in Neogene-Quaternary volcanogenic basins (19%); 3. Artesian volcanogenic basins of the Neogene-Quaternary age (8%); 4. Contact zones of the Quaternary intrusions hosted in sedimentary basins (48%); 5. Fault systems in basement rocks (10%).

Hydrothermal reservoirs in Neogene-Quaternary volcanogenic formations include: 1. Single Fault or Multiple Faults Systems (Ogiri, Hatchubaru, Sumikawa, Okuadzu, Mutnovsky (Dachny), Momotombo, Lihir, Nevada Basins and Ranges); 2. Semi-permeable Faults (Dykes) (Mac-Ban (Bulalo), Tiwi); 3. Intrusions External Contact Zones (Matsukawa, Kakkonda, Uenotai, Fushime, Tongonan, Palinpinon, Krafla, Svartsengi, Nesjavellir, Hellisheidi); 4. Volcano Conduit Zones (Hatchijo-Jima, Darajat); 5. Unwelded Tuffs and Lavas Stratigraphic Contact Zones (Yellowstone, Los-Azufres, Ahuachapan, Miravalles, El-Tatio, Olkaria, Oguni, Takigami, Wairakei, Casa-Diablo, Pauzhetsky); 6. Lava Formations (Kamojang).

The examples of the Pauzhetsky field (Kiryukhin et al, 2004, 2008) and Mutnovsky field (Kiryukhin et al, 2009) shows that high-temperature upflows and recharge downflows coincide with faults or channels, which are main conduits also for magma extrusions and volcanoes (see Figures 1 and 2). This is probably a typical case for many geothermal fields.

Geothermal fields exploration and modeling experience may apply to the NAPL-bearing volcanogenic Rogozhnikovsky reservoir in West Siberia, hosted in Triassic age rocks, which also shows multiple single faults and deep roots (Kiryukhin et al., 2008) (Figure 3).

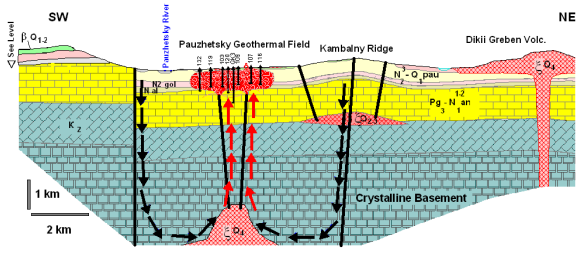

Figure 1 . Conceptual hydrogeological model of the Pauzhetsky geothermal system (Kiryukhin et al., 2008). Lithologic units: K_2 – metamorphic basement, Pg_3-N_1^{1-2} an - Miocene sandstones, N al – Neogene andesite tuffs and lavas, N_2 gol -Golyginsky Layer, N_2^3-Q_1pau – Pauzhetka Tuff, βQ_{1-2}-andesites, ξQ_{2-3}, ξQ_4 – Dacite Extrusive Complex. Black arrows: cold-water (meteoric) recharge; red arrows: ascent of heated fluids; black lines: faults; short vertical black lines: geothermal wells.

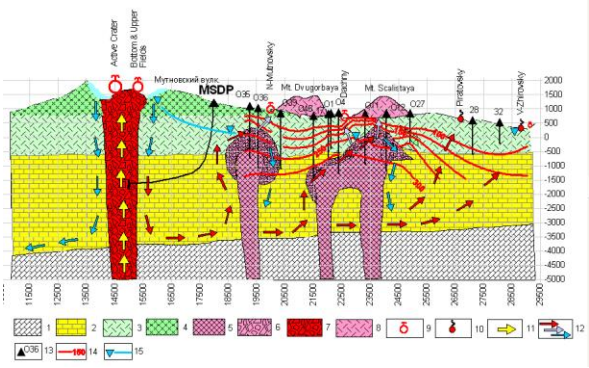

Figure 2. Conceptual model of Mutnovsky volcano - hydrothermal system: 1 – crystalline basement, 2 – Cretaceous basement and Neogene sandstones, 3- Neogene volcanogenic-sedimentary rocks, 4 – Mutnovsky stratovolcano (Q_3-Q_4), 5 – diorite intrusions, 6 – diorite intrusion contact zone, 7 – Mutnovsky volcano magma fed system, 8- rhyolite and dacite extrusions (Q_3-Q_4), 9- fumarole fields, 10 – hot springs, 11- magma and magmatic fluids, 12 – hydrothermal fluids, 13 – geothermal wells, 14 – temperature distributions, 15 – water level surface in reservoir. MSDP – proposed position of Mutnovsky Scientific Drilling Well.

INPUT DATA FOR NAPL DEPOSIT NUMERICAL MODEL

Geological Setting

Triassic volcanism in the Rogozhnikovsky area took place 242 to 258 million years ago (U-Pb dating; Korovina, 2008). Adjacent Pre-Jurassic rhyolites units penetrated by wells cover a vast area around 500 × 250 km^2 (Bochkarev et al., 2008), which indicates either significant arc volcanism or intra-plate rifting conditions at that time. As a result of this, arc and rift fracture systems maintain active fluid circulation in the West Siberian basin, which cause significant vertical disturbance of brine concentration (heavy brine upflows and diluted fluid downflow zones), thermal anomalies, and fluid pressure anomalies (low and above hydrostatic pressure zones) (Matusevich et al., 2005).

A NAPL-bearing volcanogenic reservoir exists in West Siberia, hosted in Triassic age rocks (rhyolite tuffs) at a depth between 2.5 and 2.8 km, overlaid by low-permeability clay-argillite formations. Reservoir temperatures range from 120 to 130 ^{o}C, and pressures from 290 to 310 bars.

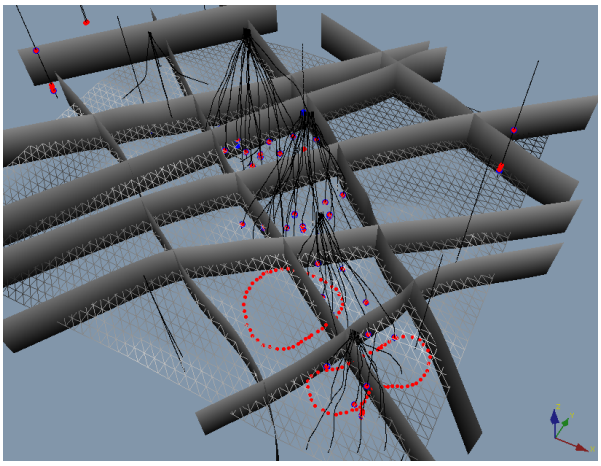

Figure 3. 3D view of Rogozhnikovsky (from Kiryukhin et al., 2008). Fractures are inferred from seismo tomography data;, red dotted lines – geoisotherms 120^{o}C at -2500 m.a.s.l., production zones – circles (NAPL – red, water – blue, NAPL above 25%+water – red with blue). Grid – roof of the Triassic volcanogenic reservoir.

Integrated analysis of the geological and geophysical data shows circulation patterns, where upflow zones are identified by positive temperature and pressure anomalies, while downflow zones are identified by negative anomalies. Those circulation patterns do not clearly fit the fracture system inferred from 3D seismotomographic data (Figure 3), while more closely coincide with the former Triassic volcanoe vents, detected by volcanic breccias penetrated by drill holes (Figure 4).

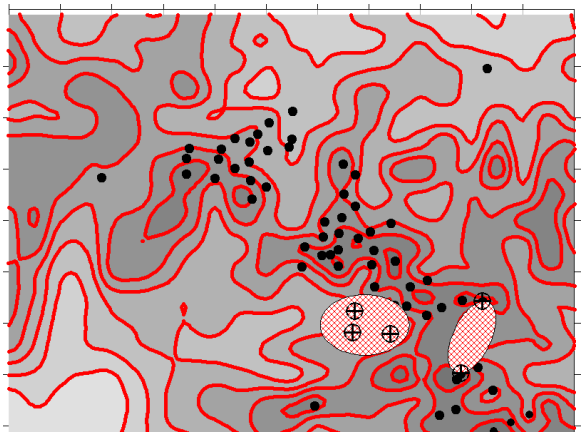

Figure 4. Surface of the volcanogenic unit (filled color, 50 m interval contours, darker at higher elevations); potential volcanic vents shown by crossed-hatched areas, wells – filled circles, wells penetrated breccias shown by crosses in circles. Grid size – 1 km.

Thermal Properties of the Reservoir Rocks Estimate

Heat test setup

Heat properties of reservoir rocks were estimated based on experiments with cylinder rock samples of 50 mm diameter and 50 mm height. The laboratory experiment setup includes a heat source (12 W) at the bottom of the cylindrical sample, a zond type temperature logger installed in the hole with 2.4 mm diameter, 10 mm from the top of the thermally insulated sample (see Figure 5). КПТ-8 paste was used to improve the thermal contact between logger and sample. A Hioki 3447-01 temperature logger was employed to register transient temperature changes (accuracy of measurements: 0.1^{o}C). All measurements took place in an underground facility with stable temperature conditions after 24 hr of delay time to reach constant initial conditions in the sample. Observational data include transient temperature records at 10 sec intervals during 5 min after the heat source was engaged.

Inverse iTOUGH2-EOS3 modeling of the Heat Tests

A cylindrical grid was used to represent the rock sample in the model (Figure 5): this grid includes 26 2-mm thick layers and 12 radial zones with logarithmically increasing radii (increment rate 1.165), where the first radius corresponds to the zond diameter of 1.2 mm, and last to the sample cylinder radius of 25 mm. Model elements are named as AI_K, where I is the layer number (from above), and K is the radial zone number (from the center). Subsequently, two domains were assigned: rock sample domain and zond domain (elements AI _1, where I=1, … ,5 up to depth 10 mm).

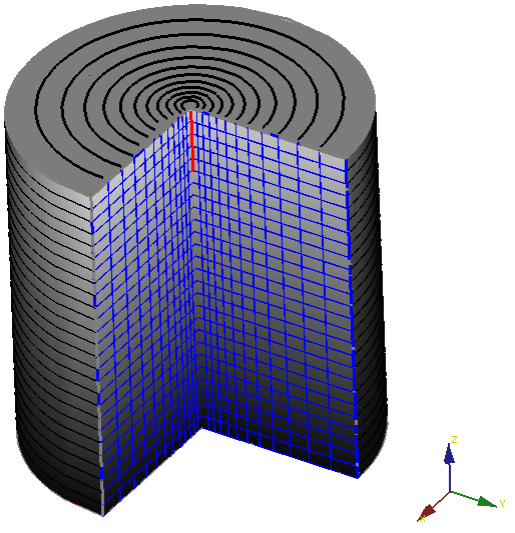

Figure 5. Numerical grid used to represent the cylinder rock sample in the model. The temperature logger is inserted at the top of the sample. The heat source is located at the bottom.

Grain density, porosity and permeability were assigned as known petrophysical parameters. Since 99% of the pore volume in the rock samples were occupied by air, the EOS-3 module for water and air was used. Correspondingly, three primary variables were used: air phase pressure P, air saturation S_g and temperature T. Initial values were assigned as P = 10^5 Pa, and S_g = 0.999 (dry samples). A linear function was used for the heat conductivity λ as a function of water saturation S_w, i.e., $\lambda = \lambda_r + (\lambda_w - \lambda_r) S_w$, where λ_w is the heat conductivity of the wet rock, and λ_r is the heat conductivity of the dry rock. The heat source was assigned to a single element B_1, which is connected to the bottom elements A_QI (I=1, … 12) with volume-proportional contact areas. The measured, transient calibration data were compared to the calculated temperature at the zond hole center (Element A3_1).

Model parameters to be estimated include heat conductivity (dry) λ_r, specific heat C_r, initial rock sample temperature T_0 and heat source rate W. Initial temperature T_0 and heating rate W were added to the parameter list because (although measured during the experiment) small variations in T_0 and W have a large impact on the predicted temperatures.

The output results of iTOUGH2-EOS3 inversions include tables of sensitivity coefficients, correlation charts, residuals, best estimates and their standard deviations. The example below shows an excerpt from the inverse modeling outputs for the 18th of 38 laboratory experiments analyzed by iTOUGH2.

```
Standard Deviations
-------------------
PARAMETER          BEST ESTIMATE      A PRIORI   CONDITIONAL       MARGINAL            C/M          1-J/P
Initial Tempera  0.1831069E+02          N/A 0.6362464E-02 0.1021403E-01          0.623          1.000
HEAT-CAP-ROCK1   0.9082472E+03          N/A 0.1329833E+01 0.1838944E+02          0.072          1.000
HEAT FLOW        0.1419087E+01          N/A 0.8870081E-02 0.1419115E+00          0.063          1.000
HEAT-COND-DRY    0.1799866E+01          N/A 0.4231720E-02 0.7494515E-01          0.056          1.000

Correlation Chart
-----------------

-1.0    -0.8    -0.6    -0.4    -0.2     0.0              0.0     0.2     0.4     0.6     0.8     1.0
  |-------|-------|-------|-------|-------|    PARAMETER    |-------|-------|-------|-------|-------|

                |-----------|-------|  Initial Tempera  |-----------|
                |           |       |                   |           |
                |           |-------|  HEAT-CAP-ROCK1   |-----------|----|
                |                                                   |    |
              |--|---------------------|     HEAT FLOW     |-----------|    |
              |  |                     |                   |                |
              |--|---------------------|   HEAT-COND-DRY   |----------------|
```

A four-parameter inversion shows acceptable correlations between the estimated parameters, which allows us to get sufficiently accurate estimates of heat conductivity (dry) (standard deviation: 0.1 W/m ^{o}C) and specific heat (standard deviation: 20 kJ/kg ^{o}C).

Figure 6 shows the comparison between measured and calculated temperatures after calibration.

Based on inversion of 38 laboratory experiments on rock samples from a well that penetrated the volcanogenic reservoir at a depth between 2580 and 2795 m, an average value of heat conductivity (dry) of 1.44 W/m ^{o}C, and an average specific heat of 850

kJ/kg ^{o}C was obtained. Accordingly to Rautman function the saturated rock has a thermal conductivity of about 1.88 W/m ^{o}C (1.44 dry rock + 0.44 water contribution).

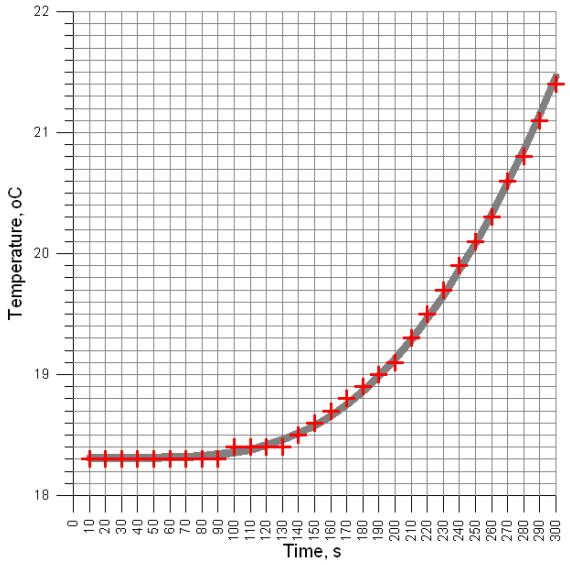

Figure 6. Comparison between measured and calculated temperatures after iTOUGH2- EOS3 calibration of the Heat Test: crosses – observational data (laboratory test #18), line – calculated temperatures.

Relative Permeabilities and Capillary Pressures

Laboratory study of relative permeabilities of five Triassic volcanogenic reservoir rock samples suggests that the van Genuchten model is appropriate for the water phase (IRP=7, RP2=0.2 – 0.5 (residual water saturation), whereas a Corey's model can be conveniently used to describe the NAPL relative permeability RP4=0.3 – 0.4 (residual NAPL saturation)) (see Figure 7).

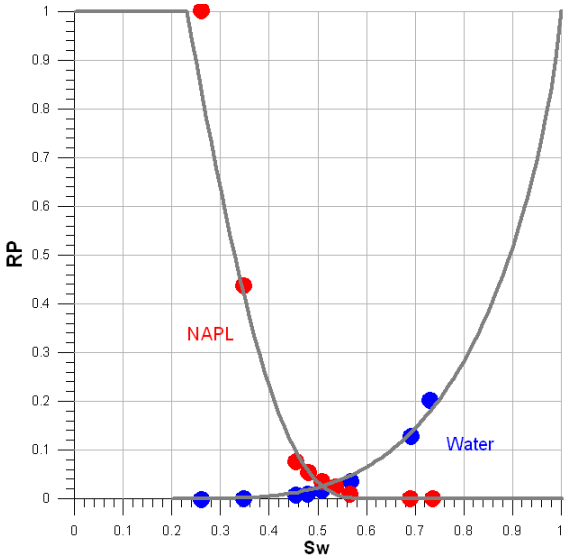

Figure 7. Experimental data (filled circles) and van Genuchten fits of NAPL and water relative permeabilities (RP) vs water saturation S_w of rock sample from volcanogenic reservoir (depth of sampling: 2640 m). Van Genuchten and Corey parameters: IRP=7, RP1=0.76 (λ), RP2=0.23 (residual water saturation), RP3=1, RP4=0.4 (residual NAPL saturation)).

A laboratory study of the capillary pressures of 126 Triassic volcanogenic reservoir rock samples suggests that the van Genuchten model (ICP=7, CP1=0.4438, CP2=S_{lr}=0.22, CP3=1/P_0=1.50E-05, CP4=Pmax=50 atm, CP5=S_{ls}=1.0) can reasonably match the experimental data (Figure 8)).

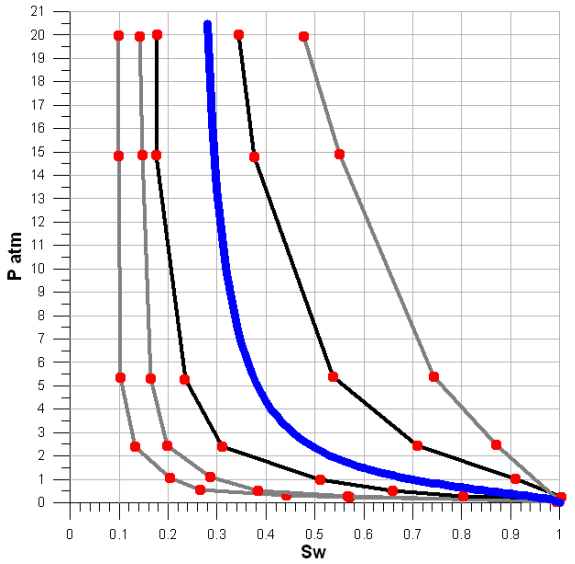

Figure 8. Experimental data ("as is", filled circles) and van Genuchten approximation (thick blue line) of capillary pressures laboratory tests of rock samples from Triassic volcanogenic reservoir. Van Genuchten parameters: ICP=7, CP1=0.4438, CP2=S_{lr}=0.22, CP3=1/P_0=1.50E-05, CP4=Pmax=50 atm, CP5=S_{ls}=1.0).

A laboratory study shows strong relationship between initial and residual NAPL saturation.

Note that West Siberian reservoirs are generally characterized by hydrophobic properties, caused by high feldspar fractions of the minerals (Matusevich et al., 2005). This means that positive oil/water capillary pressures (PC(o-w)=PC(g-w)-PC(o-w) > 0) keep the reservoir oil-wet. According to Matusevich et al. (2005) positive capillary pressures may reach 5.6 bars under some reservoir conditions, reducing the efficiency of oil recovery from the matrix by water flooding.

NUMERICAL MODELING OF NAPL DEPOSIT FORMATION IN VOLCANOGENIC ROCKS

Model Setup

TOUGH-based numerical modeling was used to understand NAPL formation and distribution in the reservoir. In a first, a 3D numerical model of the reservoir was developed, covering an area of $10 \times 8 \times 3$ km^3, discretized by a rectangular $10 \times 8 \times 30$ grid. This model covers the area shown on Figure 4.

The uppermost layer of the model (#30) was assigned at fixed state condition (10 bars, 5 ^{o}C), which corresponds to conditions approximately 100 m below land surface, where mean annual pressures and temperatures are maintained. The bottom layer of the model (#1) includes sources (potential upflow zones, where positive mass flow rate and enthalpy are assigned), sinks (potential downflow zones, where negative mass flow rates are assigned), and conductive heat flow sources in all elements of the bottom layer.

Regional lithologic characteristics used as input data for the numerical model are summarized in Table 1. These data were obtain based on core studies and correspond to matrix properties of the reservoirs. The model zonation is illustrated in Table 2.

The volcanogenic reservoir is characterized by double-porosity properties identified based on the (Fracture Micro Images (FMI) study: average vertical fracture spacing FS=26 m, fracture aperture 0.17-0.5 mm (average 0.3 mm), fracture volume fraction FV= 3.17×10^{-5}. Corresponding fracture permeability ranges from 0.23 to 1.59 D (assuming a parallel plate model). Nevertheless, a single-porosity model based on matrix properties was used as a first modeling approach.

Table 1. Regional lithologic characteristics: ρ - grain density, ϕ - porosity, k - permeability, λ - heat conductivity, SH – specific heat.

Geological index	ρ kg/m^3	ϕ	k mD	λ W/m^{o}C	SH κJ/kg^{o}C
K_2-Q caprock	2700	0.35	0.1	1.1	800
K_{1-2} aquifer J-K_1 caprock J aquifer	2700	0.20	0.19	1.2	900
Tr volcanogenic reservoir	2620	0.16	1.0	1.8	1000
Base layer	2800	0.02	0.1	2.1	1000

Table 2. Model zonation.

Geological index	Lithology	Model layers	Elevations m.a.s.l.	Domain ##
K_2-Q caprock	aleurite, clays	26-40	-1450, -50	K2Q_1
K_{1-2} aquifer J-K_1 caprock J aquifer	Sand-aleurite,	14-26	-2650, -1450	JK__1
Tr volcanogenic aquifer	Lavas, clastolavas tuffs and breccias	11-16	-2950, -2450	TR___
Basement		1-10	-3950, -2650	BASE1

Inverse iTOUGH2-EOS1 Modeling

Inverse iTOUGH2-EOS1-modeling was used to estimate heat and mass flows and permeabilities (base conductive heat flow, permeabilities of J-K_1 and K_2-Q units, upflow rate and enthalpy, and downflow rate). Model calibration was based on 41 temperature and 20 pressure calibration points. A natural-state run was performed for 10^6 years. Modeled and measured data machted relatively well, with a mean temperature deviation (bias) of -0.3 ^{o}C, a temperature standard deviation of 5.6 ^{o}C, and a mean pressure deviation of -0.03 bars, a pressure standard deviation of 8.9 bars (3% of absolute value). The uncertainty of some parameter estimates is rather high, most-likely due to over–parameterization, which leads to strong correlations, specifically between mass flows and the permeability of the K_2-Q unit). The best estimates values are: base conductive heat flow: 50.2 mW/m^2; permeabilities of the J-K_1 and K_2-Q units: 0.19 mD and 0.0011 mD, respectively;, total upflow rate: 3.6 kg/s with enthalpy of 558 kJ/kg; downflow rate: 3.6 kg/s.

Figure 9 shows corresponding pressure and temperature distributions at -2550 m.a.s.l. Upflow and downflow in the model are the same, indicating that a circulation pattern exists in the basement of volcanogenic reservoir, inspite of recharge boundaries specified on the top of reservoir.

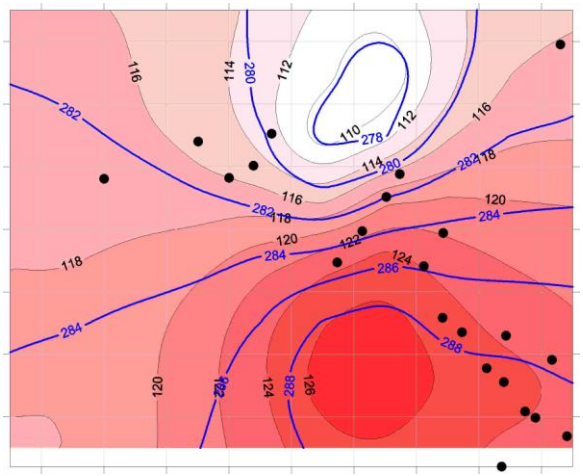

Figure 9. iTOUGH2-EOS1 natural state modeling: temperature and pressure distributions at -2550 m.a.s.l. Black filled circles – wells. Grid size – 1 km.

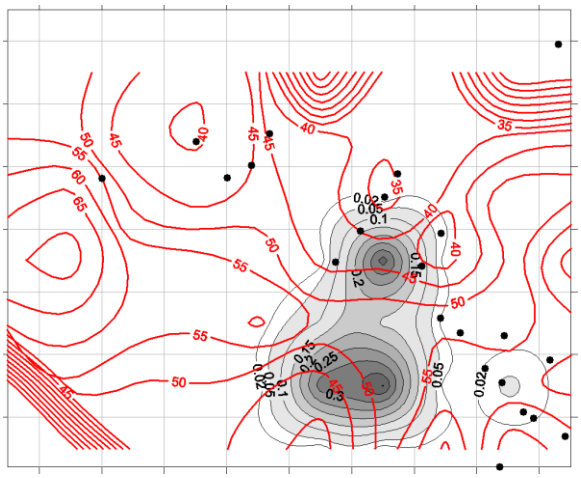

Figure 10. TOUGH2-EOS10 natural state modeling vs exploration data: modeled NAPL phase concentrations are shown as filled grey contours; exploration data NAPL phase concentrations (in %) are shown as red lines. Distributions at -2550 m.a.s.l. Grid size – 1 km.

T2VOC (direct iTOUGH2-EOS10) Natural-State Modeling

Model Setup

T2VOC (direct iTOUGH2-EOS10) modeling was used to reproduce the NAPL distribution in the volcanogenic reservoir, based on initial conditions obtained by the previous iTOUGH2-EOS1 modeling. The following scenario was used: 75.6×10^9 kg (0.24 kg/s during 10,000 years) of the NAPL was injected into the reservoir through the base upflow zones, following 90,000 years of water upflow.

Van Genuchten RP and CP functions were used with the parameters values above mentioned. Oil-wet positive capillary pressure were assigned directly in T2VOC (EOS10) by adding one line in the code: PC = -PC at the end of the van Genuchten part of the SUBROUTINE PCAP.

Modeling Results

NAPL phase saturations vs reservoir exploration data are shown in Figure 10. The modeled NAPL distribution appears as region with an S_o range from 0.05 to 0.35 inside of the zone of 45-55% NAPL phase saturation revealed by exploration. Low NAPL phase concentrations are seen in the north-east of the modeling area, which corresponds to the downflow zone.

Although this modeling example is probably not a real history of NAPL accumulation under specific reservoir conditions, nevertheless it shows the conceptual possibility of NAPL deposit accumulation in clays overlaying a Triassic rhyolite tuff reservoir fed by NAPL bearing upflows from buried volcanic vents (Figure 11).

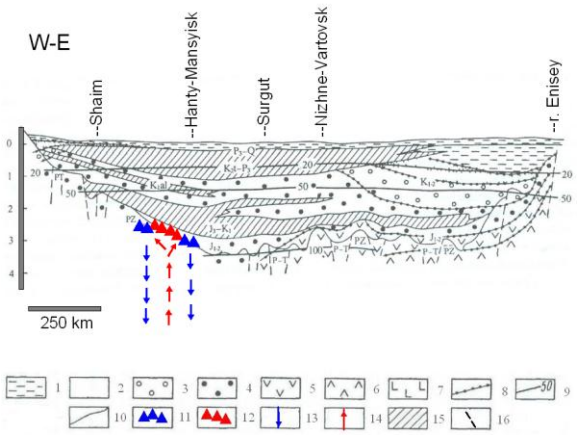

Figure 11. Cross section of West Siberian basin (from V.A. Kiryukhin, 2005) with added schematic indication of Triassic volcanogenic reservoir and possible circulation patterns along former volcanoe vents. Legend: 1 – 7 hydrogeochemical zonation: mineralization < 1 g/l (1), 1-3 g/l (2), 3-10 g/l (3), 10-35 g/l (4), 35-70 g/l (5), 70-150 g/l (6), 150-375 g/l (7); 8 – hydrogeochemical zone boundaries; 9 – geoisotherms, ^oC; 10- lithological boundaries; 11 - water filled volcanogenic reservoir;12 – NAPL filled volcanogenic reservoir, 13 – separated water downflow channels; 14 – NAPL bearing ascending fluid channels; 15 – clay caprock units; 16 – faults.

Future Study

We plan to extend the model domain to include the entire field, making a short-term study of the natural state conditions of the Rogozhnikovsky reservoir to understand the existing NAPL body dynamics under

the current temperature distributions and upflow-downflow conditions.

In parallel to this, a more detailed model approach for different exploitation scenarios is needed. This study should include well-by-well grid generation, taking into account double-porosity properties, spatial distributions of reservoir parameters (such as matrix porosity, permeability, initial NAPL saturations) as confirmed by extensive geophysics well logging, seismo tomography and FMI, as well as extensive core petrophysical studies. NAPL production and water production history matching is also planned. It would be necessary to consider in a more rigorous way the effects of brine properties (density, viscosity) that are functions of salt concentration. Future drilling locations and how to improve the efficiency of NAPL recovery from oil-wet volcanogenic reservoir conditions remain the primary challenge.

CONCLUSIONS

1. Based on analyses of hydrothermal reservoirs in recent volcanic areas, a conceptual model of NAPL reservoir formation in old volcanogenic formations was hypothesized. It was assumed that these reservoirs may use former volcanoes vents buried under sedimentary basins as channels of ascending NAPL-bearing fluids.

2. iTOUGH2-EOS3 modeling was used to estimate heat properties of the volcanogenic formation based on laboratory heat tests on 38 rock samples. iTOUGH2 inversions show the possibility of simultaneously estimating heat conductivity (dry) and specific heat with reasonable accuracy. Mean heat conductivity (dry) and specific heat values of 1.4 W/m^{o}C and 850 kJ/kg ^{o}C were obtained.

3. Conceptual iTOUGH2-EOS1 natural-state modeling based on measured pressure-temperature calibration data is an effective tool to verify deep seated circulated mass flow conditions, base conductive heat flow and permeabilities, nevertheless just three of six estimated parameters are independent enough for accurate estimations. Hence, best estimates obtained: base conductive heat flow: 50.2 mW/m^2; permeabilities of the J-K_1 and K_2-Q: 0.19 mD and 0.0011 mD, respectively; total upflow rate: 3.6 kg/s with an enthalpy of 558 kJ/kg; downflow rate: 3.6 kg/s – assumed to be one of possibilities.

4. Conceptual T2VOC (direct iTOUGH2-EOS10) modeling was used to demonstrate possibility oil deposits could accumulate in clay overlaying Triassic volcanogenic reservoirs, fed by NAPL-bearing upflows from buried volcanic vents.

ACKNOWLEDGMENTS

The author expresses gratitude to Dr. A. Battistelli and Dr. S. Finsterle for their helpful comments and suggestions. This work was supported by RFBR project 09-05-00605-a.

REFERENCES

Bochkarev V.S., Brekhuntsov V.M., Lukomskaya K.G. On the Issue of the Permian-Triassic in Western Siberia, Gornye Vedomosti 2, p. 7-17 (in Russian), 2009.

Falta R., Pruess K., Finsterle S., Battistelli A. T2VOC User's Guide LBNL-36400, 1995.

Finsterle S. iTOUGH2 User's Guide, LBNL-40040, 1999.

Kiryukhin A.V., Yampolsky V.A., Modeling Study of the Pauzhetsky Geothermal Field, Kamchatka, Russia, Geothermics, v.33, No.4, p. 421-441, 2004.

Kiryukhin A.V. Modeling of the Dachny Site Mutnovsky Geothermal Field (Kamchatka, Russia) in Connection with the Problem of Steam Supply for 50 MWe Power Plant, Proceedings World Geothermal Congress 2005 Antalya, Turkey, 24-29 April 2005, 12 p.

Kiryukhin A.V., Nikolaeva E.V., Baturin A.Y. Comparative Analysis Geological and Thermohydrodynamic Models of Oil and Geothermal Deposits Hosted in Volcanogenic Rocks of Different Age, Proc. All Russia Conference "Earth Degasation: Geodynamics, Geofluids, Gas and their Para genesis" Moscow, p. 204-206 (in Russian), 2008.

Kiryukhin A.V., Asaulova N.P., Finsterle S. Inverse modeling and forecasing for the exploitation of the Pauzhetsky geothermal field, Kamchatka, Russia, Geothermics, V. 37, p. 540-562, 2008.

Kiryukhin A.V., Kiryukhin V.A. Manukhin Y.F. Hydrogeology of Volcanogenic Areas, S-Petersburg, Nauka Publ., 396 p. (in Russian), 2009.

Kiryukhin V.A. Regional Hydrogeology, S-Petersburg Mining Inst., 343 p, 2005.

Matusevich V.M., Rylkov A.V., Ushatinsky I.N. Geofluid Systems and Problems of Oil and Gas Deposits Distributions in West Siberia Megabasin, Tumen State Oil University, 224 p. , 2005

Pruess, K., Oldenburg, C., Moridis, G., TOUGH2 User's Guide, Version 2.0. Lawrence Berkeley National Laboratory report LBNL-43134, Berkeley, CA, USA, 198 pp, 1999.